www.czasopisma.pan.pl PAN POLSKA AKADEMIA NAUK www.journals.pan.pl

Arch. Min. Sci. **63** (2018), 4, 1007-1025

Electronic version (in color) of this paper is available: http://mining.archives.pl

DOI 10.24425/ams.2018.124990

MAREK CAŁA*, KATARZYNA CYRAN*#, MICHAŁ KOWALSKI*, PAWEŁ WILKOSZ**

INFLUENCE OF THE ANHYDRITE INTERBEDS ON A STABILITY OF THE STORAGE CAVERNS IN THE MECHELINKI SALT DEPOSIT (NORTHERN POLAND)

WPŁYW WKŁADEK ANHYDRYTOWYCH NA STATECZNOŚĆ KAWERN MAGAZYNOWYCH W ZŁOŻU SOLI KAMIENNEJ MECHELINKI (PÓŁNOCNA POLSKA)

This paper presents a complex study of anhydrite interbeds influence on the cavern stability in the Mechelinki salt deposit. The impact of interbeds on the cavern shape and the stress concentrations were also considered. The stability analysis was based on the 3D numerical modelling. Numerical simulations were performed with use of the Finite Difference Method (FDM) and the FLAC3D v. 6.00 software. The numerical model in a cuboidal shape and the following dimensions: length 1400, width 1400, height 1400 m, comprised the part of the Mechelinki salt deposit. Three (K-6, K-8, K-9) caverns were projected inside this model. The mesh of the numerical model contained about 15 million tetrahedral elements.

The occurrence of anhydrite interbeds within the rock salt beds had contributed to the reduction in a diameter and irregular shape of the analysed caverns. The results of the 3D numerical modelling had indicated that the contact area between the rock salt beds and the anhydrite interbeds is likely to the occurrence of displacements. Irregularities in a shape of the analysed caverns are prone to the stress concentration. However, the stability of the analysed caverns are not expected to be affected in the assumed operation conditions and time period (9.5 years).

Keywords: storage caverns, stability analysis, anhydrite interbeds, 3D numerical modelling

W artykule przedstawiono kompleksowe studium wpływu wkładek anhydrytowych na stateczność kawern magazynowych w złożu soli kamiennej Mechelinki. Rozważany był także wpływ wkładek anhydrytowych na kształt kawern magazynowych i koncentrację naprężeń. Analizę stateczności przeprowadzono z wykorzystaniem metod modelowania numerycznego. W symulacjach numerycznych została zastosowana metoda różnic skończonych i program FLAC3D v. 6.00. W celu wykonania symulacji numerycznych zbudowano model numeryczny analizowanego obszaru. Model numeryczny w kształcie sześcianu i wymiarach 1400 × 1400 × 1400 m obejmował część złoża Mechelinki oraz trzy kawerny magazynowe (K-6, K-8, K-9). Siatka modelu składała się z 15 milionów teraedrycznych elementów.

* AGH UNIVERSITY OF SCIENCE AND TECHNOLOGY, FACULTY OF MINING AND GEOENGINEERING, KRAKOW, POLAND, AL. MICKIEWICZA 30, 30-059 CRACOW

** GAS STORAGE POLAND SP. Z O. O., AL. JANA PAWŁA II 70, 00-175 WARSAW

Corresponding author e-mail: kcyran@agh.edu.pl

Występowanie wkładek anhydrytowych w obrębie pokładu soli kamiennej przyczyniło się do redukcji średnicy i nieregularności kształtu analizowanych kawern magazynowych. Wyniki modelowania numerycznego 3D wykazały, że strefy kontaktu pomiędzy warstwami soli kamiennej i wkładkami anhydrytowymi są podatne na występowanie przemieszczeń. Ponadto, obszary koncentracji naprężeń są związane z nieregularnością kształtu komór magazynowych. Symulacje numeryczne wykazały, że stateczność analizowanych komór w przyjętych warunkach eksploatacji i analizowanym 9.5-letnim okresie nie zostanie naruszona.

Słowa kluczowe: kawerny magazynowe, analiza stateczności, wkładki anhydrytowe, modelowanie numeryczne 3D

1. Introduction

Stability analysis is performed in order to predict the cavern performance in specific geological and mining conditions as well as to understand the effect of the cavern shape and size on the stability conditions. In bedded salt formations, cavern design and stability assessment requires the consideration of interbedded rocks composed of claystones, carbonates, sulphates and K-Mg salt minerals. Interbeds are characterised by the distinct level of solubility, which results in the occurrence of irregularities in the cavern shape such as overhanging blocks on the cavern wall or shrinks in "waist" or "neck". (Warren, 2006). The structural stability of caverns in bedded salt depends on the strength and deformation characteristics of the salt and nonsalt beds surrounding and overlying the cavern (deVries et al., 2005). Creep deformations between the salt rock and interbeds can influence the storage operations and in the long run can contribute to gas migration (Xiong et al., 2015).

Stability analyses of caverns in bedded salt formations were performed by many authors (Zhang et al., 2015a, b; Li, 2015; Han et al. 2007). The cavern roof stability in a bedded rock salt formation was studied by Bruno (2005), Bruno et al. (2005) and deVries et al. (2005). The influence of interlays on the storage operations was analysed by Cosenza et al. (1999) and Consenza & Ghoreychi (1999). Creep characteristics of rock salt in bedded salt formations and the effect of the creep deformation on the surrounding rocks was studied by Minkley & Muhibauer (2007). The impact of the interbeds in bedded rock salt deposits on cavern shape was studied by Li et al. (2017), Wang et al. (2013), Sobolik & Ehgartner (2006). The mudstone and clay interbeds influence on the cavern stability was studied by Yang et al. (2005), Li et al. (2007), Yu & Liu (2015).

In this paper, a complex study of anhydrite interbeds influence on the cavern stability was performed. Deformations resulting from the differences in the mechanical parameters of rock salt and anhydrite interbeds were studied as well as their influence on the surrounding rocks. Moreover, the impact of interbeds on the cavern shape, as well as the stress concentrations resulting from the shape irregularities and the distinction between the mechanical parameters of rock salt and anhydrite were analysed.

2. Outline of the geology of the studied area

The Zechstein salt bearing formation comprises the area of the Baltic coast from Łeba to the Hel peninsula. In this area, the Zechstein formation has developed in three cyclothems PZ1, PZ2 i PZ3. Cyclothems PZ2 and PZ3 are developed partially and spread unevenly. The rock salt (Na1) occurs only in cyclothem PZ1 (Czapowski & Bukowski, 2010).

The Mechelinki salt deposit is situated in the northern part of the Gdańsk bay, where the salt beds thickness is the highest (Czapowski et al., 2007; Lankof et al., 2016). The salt deposit comprises an area of 6.4 km^2 and it is a pentagonal shape, measuring 3.2 km × 2.0 km (Fig. 1).

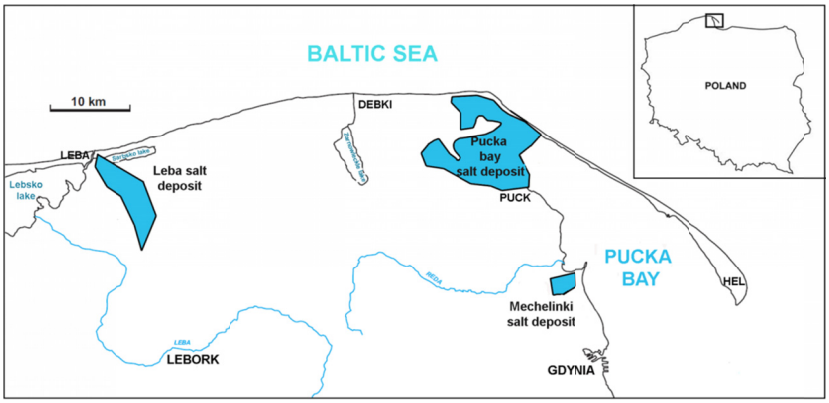

Fig. 1. Location of Mechelinki salt deposit (after Czapowski & Bukowski, 2010; Wilkosz et al., 2012)

The top of the rock salt beds occur from the depth of 946.2 m below sea level (b.s.l.) to 996.1 m b.s.l. (Fig. 2). The thickness of salt beds changes from 123.6 m to 285.9 m. The rock

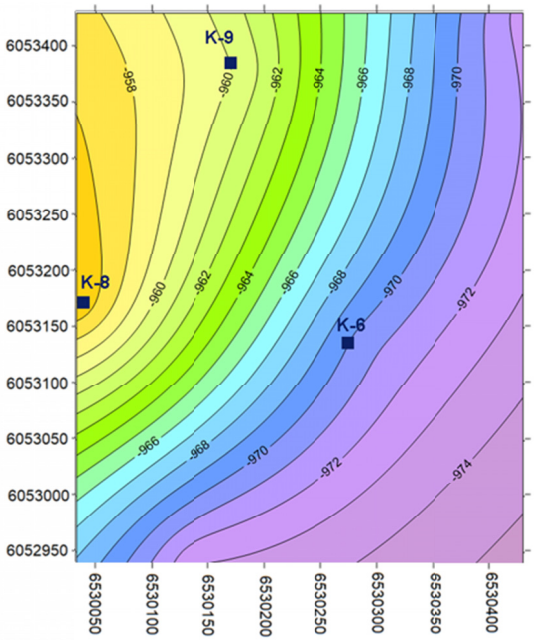

Fig. 2. Location of the K-6, K-8, K-9 caverns in the background of the of salt beds roof depth in Mechelinki salt deposit

salt is mainly fine- and medium-grained with NaCl content varying from 96,7 to 97,8%. The impurities are mainly anhydrite, which is dispersed within halite crystals or occurs as the laminae (thickness of 1-8 mm). There are also thin (from a few to 20 cm) layers or packets of crystal salts. The salt beds are underlain and overlain by anhydrite layers (the lower anhydrite – A1d and the main anhydrite – A1g) with thickness ranges from about 1.5 to 20 m. There are two anhydrite interbeds A1śr1 and A1śr2 that occur within the rock salt layer with a thickness reaching 0.5 m. The salt beds lie concordantly on the lower anhydrite (A1d) and dip in SSE (max. 10°).

The following stratigraphic units of the PZ1 cyclothem underlie the salt beds and the lower anhydrite: Kupferschiefer (T1), Zechstein Limestone (Ca1) as well as the Rotliegend sediments (mainly sandstone and conglomerates) and the Silurian sediments. The salt beds and the main anhydrite are covered by the sediments of the PZ2 and PZ3 cyclothems, mainly limestones, sulphates and silts which overlie the salt beds. The Zechstein sediments are overlain by the Triassic, Jurassic, Cretaceous and Kenozoic strata (Czapowski et al., 2007).

3. Methods and conditions of the stability analysis

The stability analysis of the storage caverns in the Mechelinki salt deposit was based on numerical modelling. In numerical modelling, the nature of a rock mass is characterised by mathematical models, whereas the physical processes are represented by differential equations. The relevant mechanisms and constitutive laws with the associated variables and parameters are applied during the numerical model conceptualisation. Complex problems are solved by computational simulations (Jing, 2003).

3.1. Methods

In order to assess the stability conditions of the caverns in the Mechelinki salt deposit, the Finite Difference Method (FDM) and the FLAC3D v. 6.00 software (Itasca Consulting Group) was used. FLAC 3D is a valuable tool in solving geomechanical and geotechnical problems, including rheological phenomena. FLAC modelling techniques are useful in the prediction and the monitoring of cavern stability in salt deposits because the program can simulate the behavior of materials that exhibit creep. FDM is an approximate method for solving differential equations. This method can be applied to problems with different shapes, different boundary conditions and different materials. Shapes and modelled objects are projected by polyhedral zones that form a 3D grid. The behavior of these zones in response to the applied forces or boundary restraints is described by a (stress-strain law) constitutive model (Swift & Reddish, 2005; Zhang et al., 2015a).

3.2. The geometry of caverns

The analysed caverns (K-6, K-8, K-9) were projected in the numerical model as a 3D geometric shape. The geometry and the dimensions of the caverns in numerical modelling were simulated, based on the echometric survey data. Generally, the shape of analysed caverns in the Mechelinki salt deposit is cylindrical and enlarged in the lower part, but there are some irregularities connected to the geological structure and the lithology of salt beds. The main irregularities are connected to the occurrence of two anhydrite interbeds within the rock salt beds. In the

vertical cross-section of all analysed caverns, significant changes in the diameter ranges from a few, to even a dozen or so meters are visible (Fig. 3). This reduction in diameter of caverns was caused by the presence of anhydrite interbeds. In a 3D view, the caverns seem to be tilted towards SSE (Fig. 4). This tilt complies with the dipping direction of the salt beds. Moreover, some small irregularities in a shape of the caverns may be connected to the occurrence of crystal salt layers or packets.

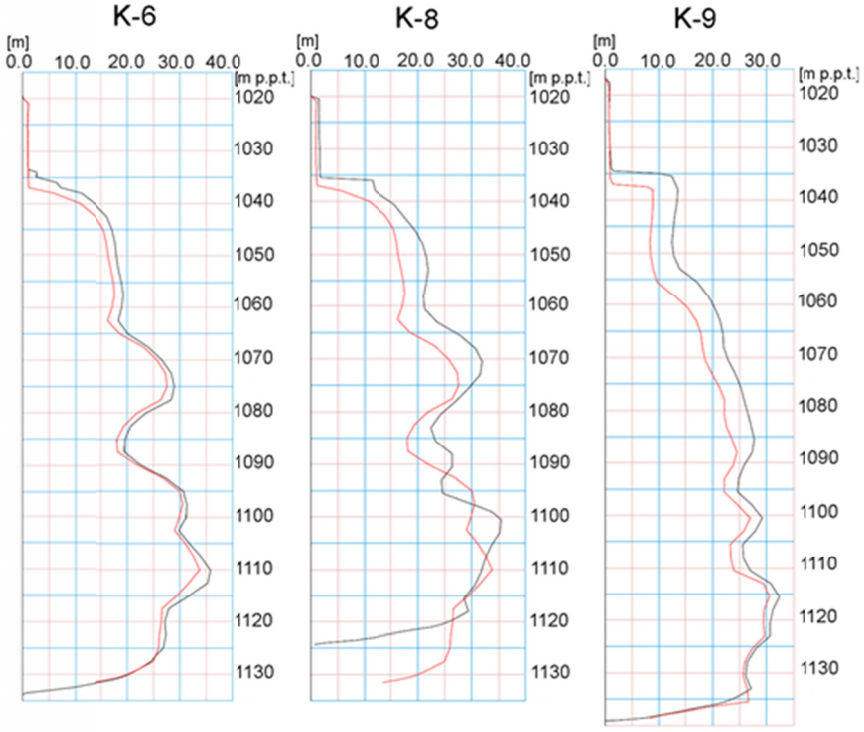

Fig. 3. Irregularities in the caverns shape (vertical cross-section) based on the echometric survey data

3.3. The numerical model of salt deposit and caverns

In order to perform a stability analysis, a numerical model of the rock mass surrounding the analysed caverns was built. The numerical model simplifies to an acceptable extent the geological and mining conditions in salt deposit. The numerical model comprised the part of the Mechelinki salt deposit that is in the shape of cuboid and of the following dimensions: length 1400, width 1400, height 1400 m (Fig. 5). The geological structure of the deposit was projected based on the description of the geological cores and the geophysical logs (Brańka et al., 2014). The model extended vertically from the ground surface to 1400 m below sea level (b.s.l.). Three caverns were projected inside this model. The mesh contained about 15 million tetrahedral elements. Elements dimensions at the cavern sidewalls were smaller (about 1 m) so that they could accurately represent the caverns shape and stress conditions. Outside the cavern, the sidewalls elements

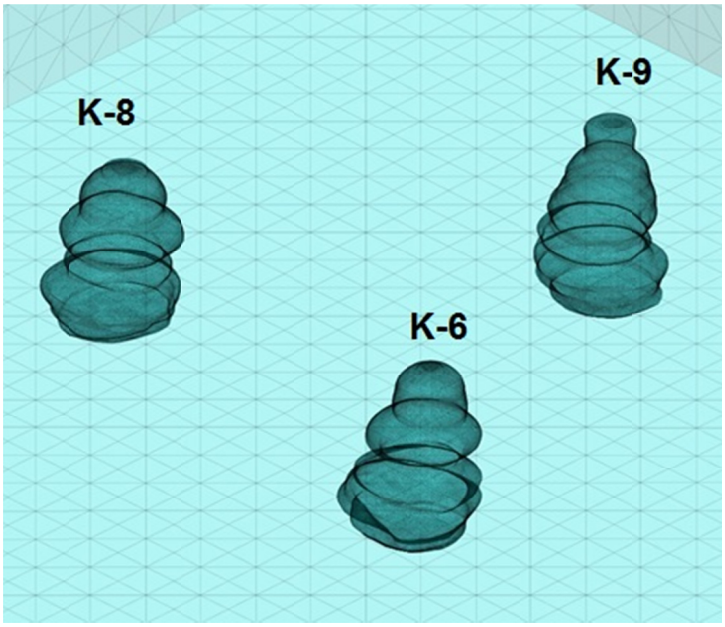

Fig. 4. A shape of the caverns projected in a 3D numerical model

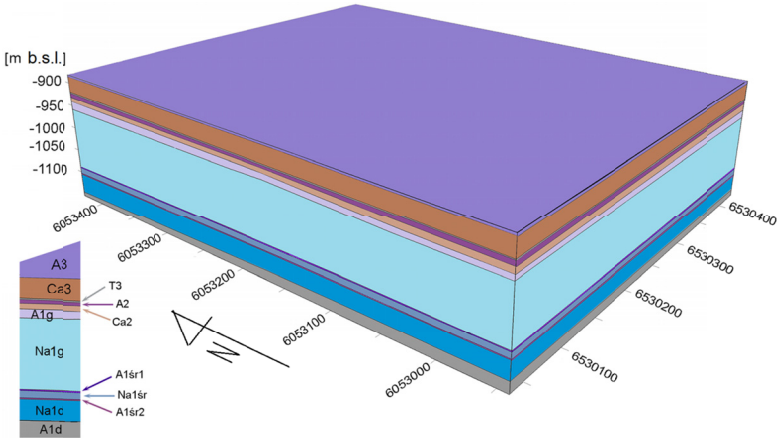

Fig. 5. The geological structure projected in the numerical model that comprises analysed part of the Mechelinki salt deposit. This figure presents the part of the numerical model which includes the rock salt and the underlying anhydrite and the overlying Zechstein beds

were bigger (about 20 m). The boundary conditions of the numerical model were introduced by blocking the displacement in the perpendicular direction to the bottom and the side planes. The value of the hydrostatic stress changed within the depth from zero at the surface to 33.6 MPa at the bottom of the 3D model.

3.4. Material models and parameters

The mechanical behavior of the rock mass surrounding the analysed caverns was simulated based on the constitutive models and the mechanical parameters of the rock salt and the nonsalt rock. The constitutive models of the materials describe the stress-strain behavior in response to the applied loads. In numerical modelling, two constitutive models were applied to describe the mechanical response of the surrounding rocks on the storage cavern: a two-component Norton Power Law with a Mohr-Coulomb plasticity criterion, and the Mohr-Coulomb elastic-plastic model. These models were chosen as they reflect the complexity of mining and the geological conditions, but also because they simulate the elastic-plastic response of rocks and the viscoelastic-plastic behavior of rock salt.

The parameters required specifying the material strength and the mechanical behavior for the nonsalt rocks and the rock salt were determined in laboratory tests. Four types of materials were distinguished for the needs of the numerical modelling: rock salt, anhydrite, rocks e.g. dolomite or limestone and soils. The parameters applied to the numerical calculations were based on the results of the laboratory tests and literature data (Tab. 1).

TABLE 1

Mechanical parameters applied in the geomechanical analysis

Parameters	Anhydrite	Rocks	Soils	Rock salt
Bulk density [kg/m^3]	24	24	24	24
Young's modulus [MPa]	12 000	10 000	100	5 000
Poisson's ratio [-]	0.20	0.25	0.25	0.45
Cohesion [kPa]	4 000	5 000	10	10 990
Internal friction angle [°]	35	40	25	36.4
Tensile strength [kPa]	1 000	2 000	10	2 000

In addition, creep parameters for rock salt (determined in laboratory tests and calculated based on the Norton Power law) were n = 5.0 and $A = 1.08 \cdot 10^{-45}$ $Pa^{-5.0}$ s^{-1}.

3.5. The conditions of stability analysis

Stability analyses were carried out for a period of 9,5 years, and consisted of three phases: leaching, 4 years when the caverns were filled with brine and 5 pressure cycles when the cavern pressure oscillates between the minimum 4 MPa to the maximum 17.5 MPa. Numerical analysis was performed for each cavern separately and for the group of all three caverns altogether as well (K-6, K-8, K-9).

A stability assessment of the caverns included the determination of the strength/stress ratio, the displacements, the von Mises stress and the vertical stress. The strength/stress ratio analysis has indicated the endangered area in the sidewalls of all analysed caverns and in its surrounding. The strength/stress ratio equal to 1.0 implies a cavern failure. Consequently, the strength/stress ratio is called a factor of safety. Displacements at the sidewalls as well as at the bottom and the roof of the caverns in different cross-sections were analysed. The displacements illustrate the decrease in the cavern volume with time (cavern convergence) caused by the salt creep. Moreover, the von Mises stress and the vertical stress were calculated in order to evaluate the stability

of the pillars between the caverns, as well as over the cavern roof and under the cavern bottom. The von Mises stress is the equivalent effective stress that is related to the creep rate within the primary and the secondary creep stages. The vertical stress represents overburden pressure on the analysed caverns.

The results of the stability analysis were presented in the form of maps (Figs. 6-13). The maps show, with the help of a coluor scale, the values of the analysed factors: the displacements, the strength/stress ratio, the vertical and the von Mises stress in the relevant time period. Different colours represent different values of each factor, for instance, the dark blue colour represents the value 2.5 of the strength/stress ratio in the maps.

4. The results of the stability assessment

Numerical modelling and a stability assessment of the cavern were performed twice: immediately after the cavern leaching (cavern completion period) and 9.5 years after the leaching (operation period). Moreover, the analyses concerning the stability of the safety pillars (between the caverns, the bottom and the roof pillars) were performed for twice: immediately after the leaching (the cavern completion period) and 4 years after the leaching (brine storage period).

In the first case (immediately after the leaching) the numerical analysis performed for each cavern separately revealed that the maximum displacements in the caverns are expected to reach: 10.28 cm for the K-8 cavern, 9.83 for the K-6 cavern and 9.42 for the K-9 cavern. It should be underlain that these maximal values of displacements were indicated locally in all three caverns (Fig.6). The recorded displacements are located in the zones where a diameter of the caverns was reduced and irregularities in the caverns shape occur. Moreover, these zones correlate with the contact between the anhydrite interbeds and the rock salt. These zones are represented by two small areas of maximum displacements at the sidewalls of the caverns K-8 and K-9, as well as one zone for cavern K-6. At the end of the cavern completion period, the described displacement zones are predicted to expand. Consequently, the maximal values of the displacements are predicted to increase to: 69.9 cm for the K-6 cavern, 68.3 cm for the K-8 cavern and 68.7 cm for the K-9 cavern (Fig. 7). In addition, the third zone connected with the reduction in the cavern diameter is visible in the sidewalls of the K-8 cavern. It should be pointed out that the displacement values are differentiated in the sidewalls of each of the analysed caverns. The maximal value of the displacements in the most areas of each of the cavern sidewalls is expected to reach about 5.0-7.0 cm in the first analysed period, and about 40.0-50.0 cm at the end of the operation period. However, the displacement zones are characterised by that that the maximal values were indicated locally in both analysed periods.

Moreover, the numerical analysis carried out for the group of all three caverns determined similar maximal values of displacements: 9.62 cm at the end of the completion period and 23.3 cm at the end of the brine storage period. The maps (Fig. 8) clearly show that the displacement zones correlate with the area of contact between the rock salt beds and the anhydrite interbeds A1śr1 and A1śr2.

Furthermore, the von Mises stress is distributed irregularly in the rock mass around each analysed cavern. The average value of the von Mises stress is expected to reach 6.0-7.0 MPa in the rock mass surrounding the caverns at the end of operation period (Fig. 9) However, the local areas of stress concentration were indicated in each analysed cavern. They are connected

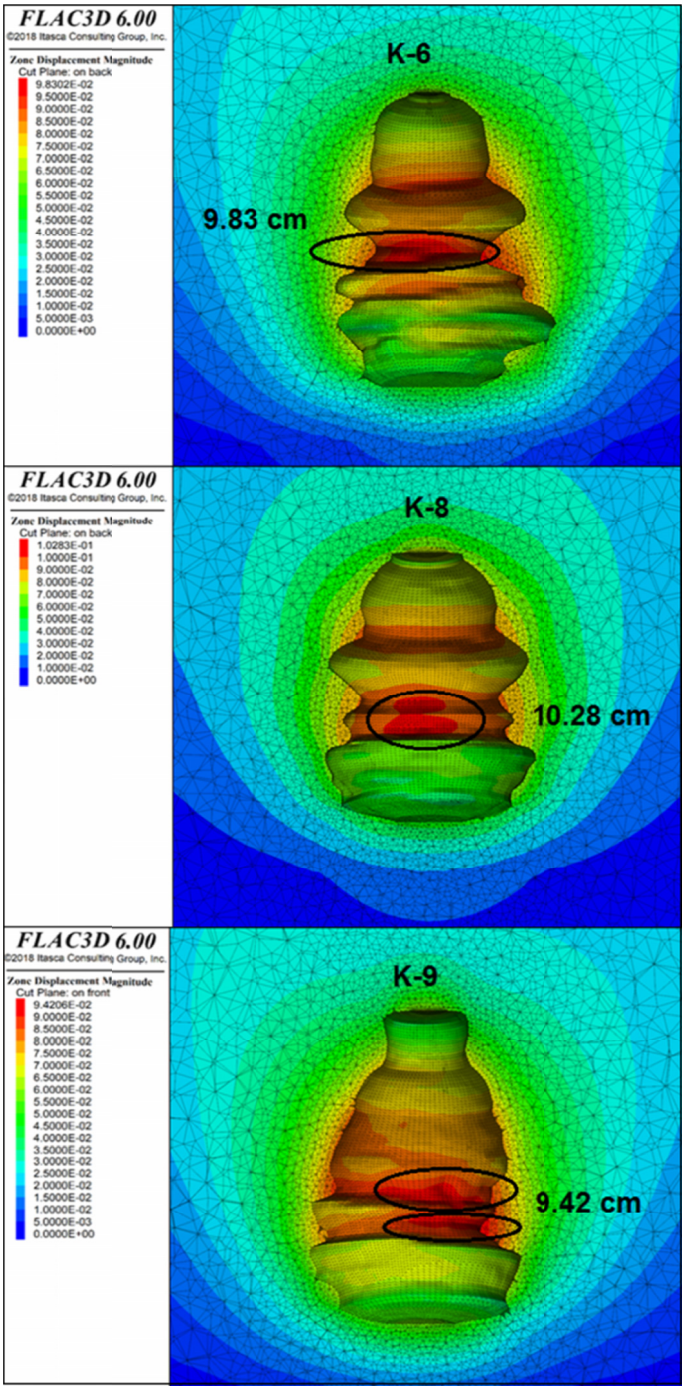

Fig. 6. Maximal values of displacements for each cavern immediately after leaching. The highest values of displacement are circled in black

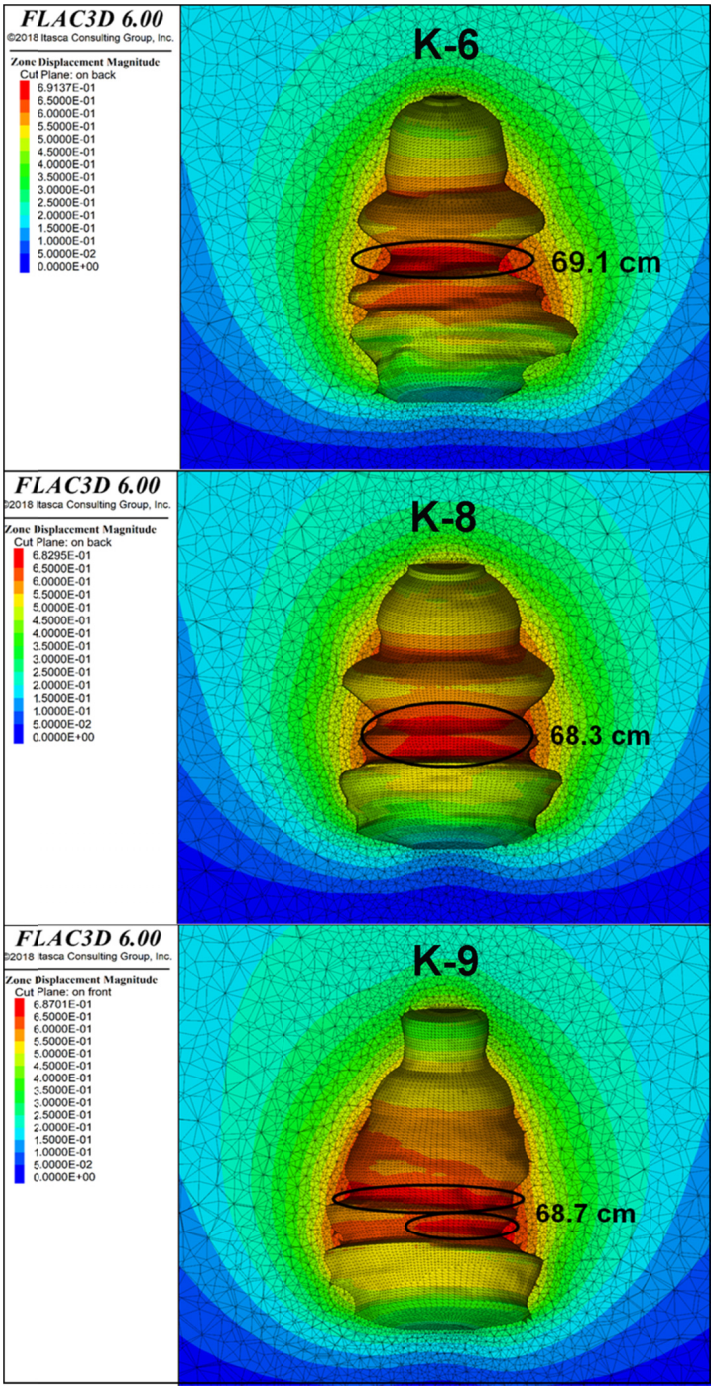

Fig. 7. The maximal values of displacements for each cavern at the end of the operation period (after 9.5 years). The highest values of displacement are circled in black

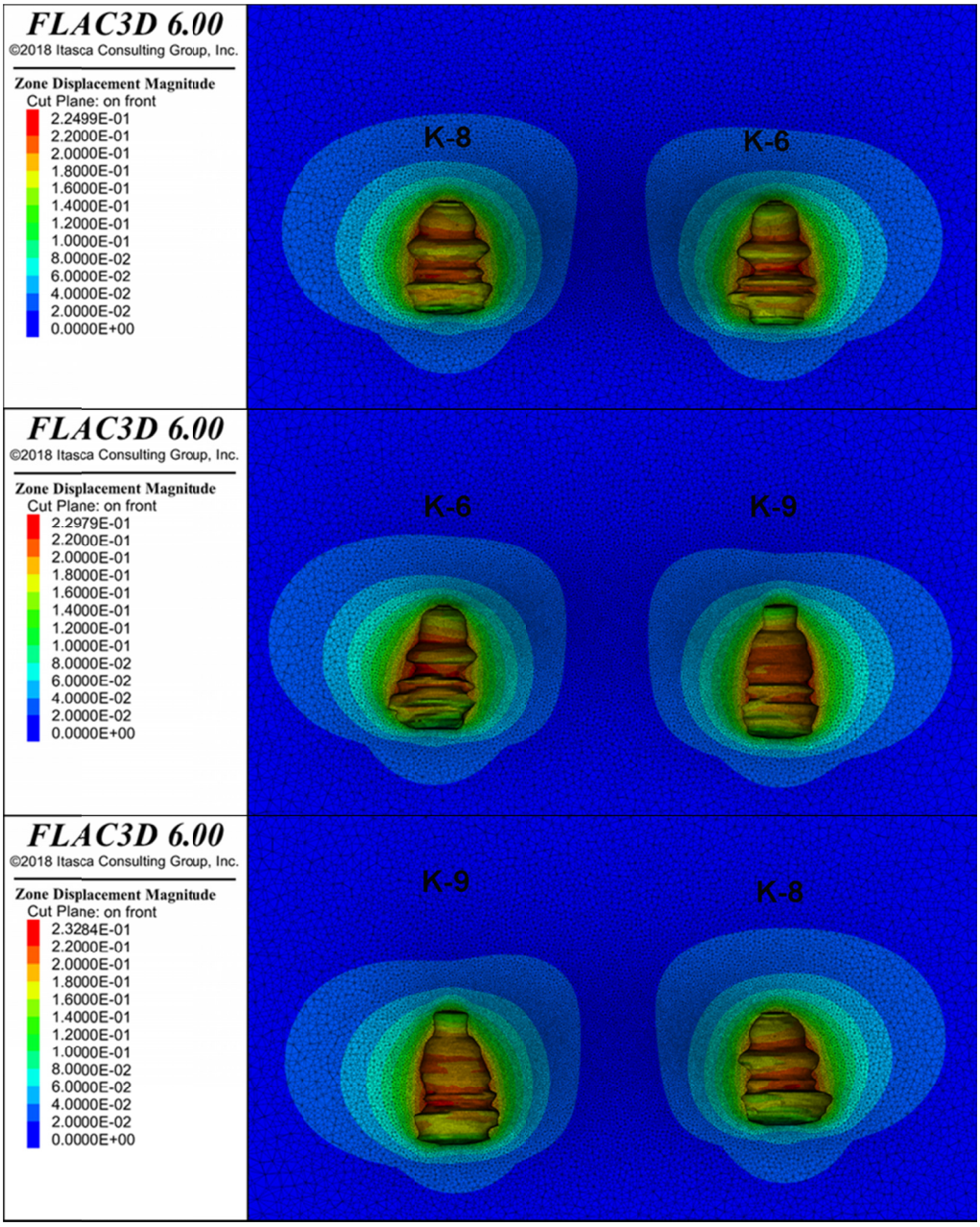

Fig. 8. The maximal values of displacements for the group of caverns at the end of the brine storage period (after 4 years). Displacements above 20 cm are marked in red

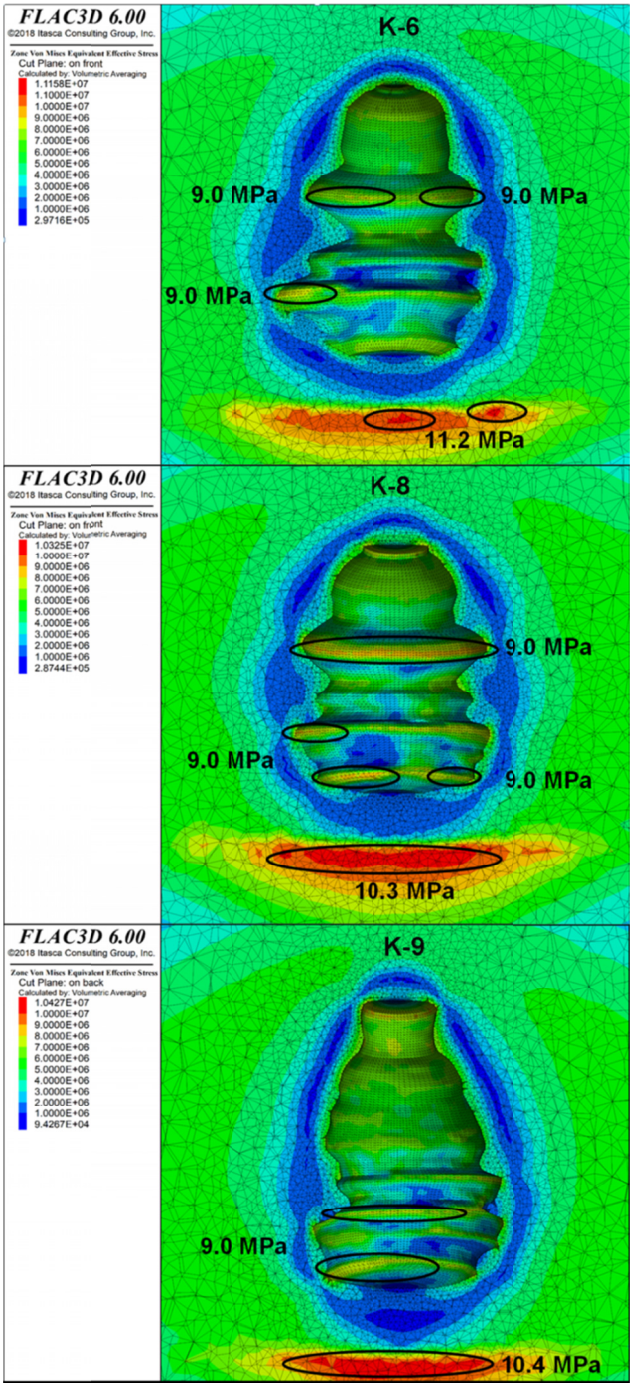

Fig. 9. Maps of the von Mises stress for each cavern at the end of the operation period (after 9.5 years). The highest values of the von Mises stress are circled in black

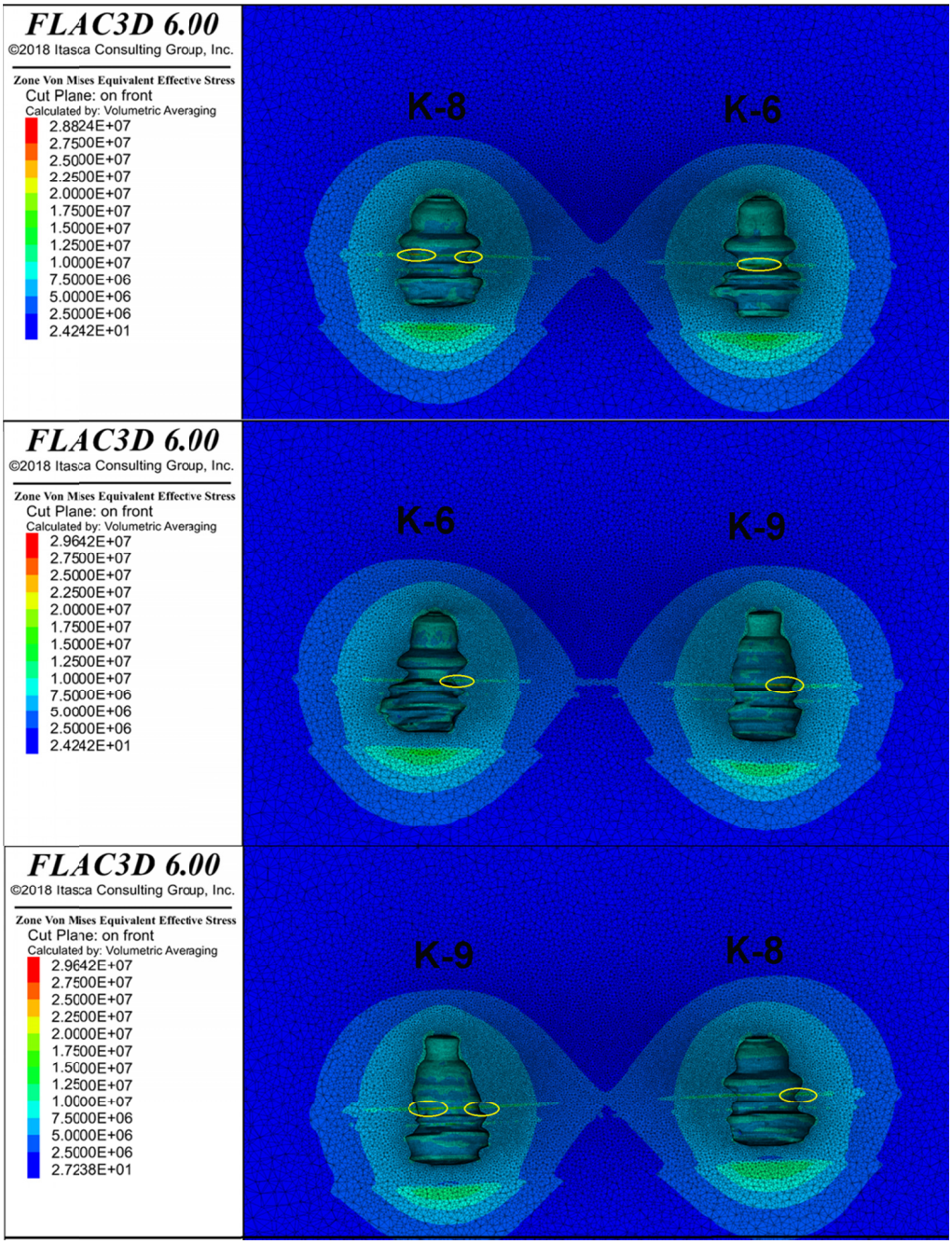

Fig. 10. Maps of the von Mises stress for a group of caverns at the end of the brine storage period (after 4 years). Areas characterised by the von Mises stress of 25.0 MPa are circled in yellow

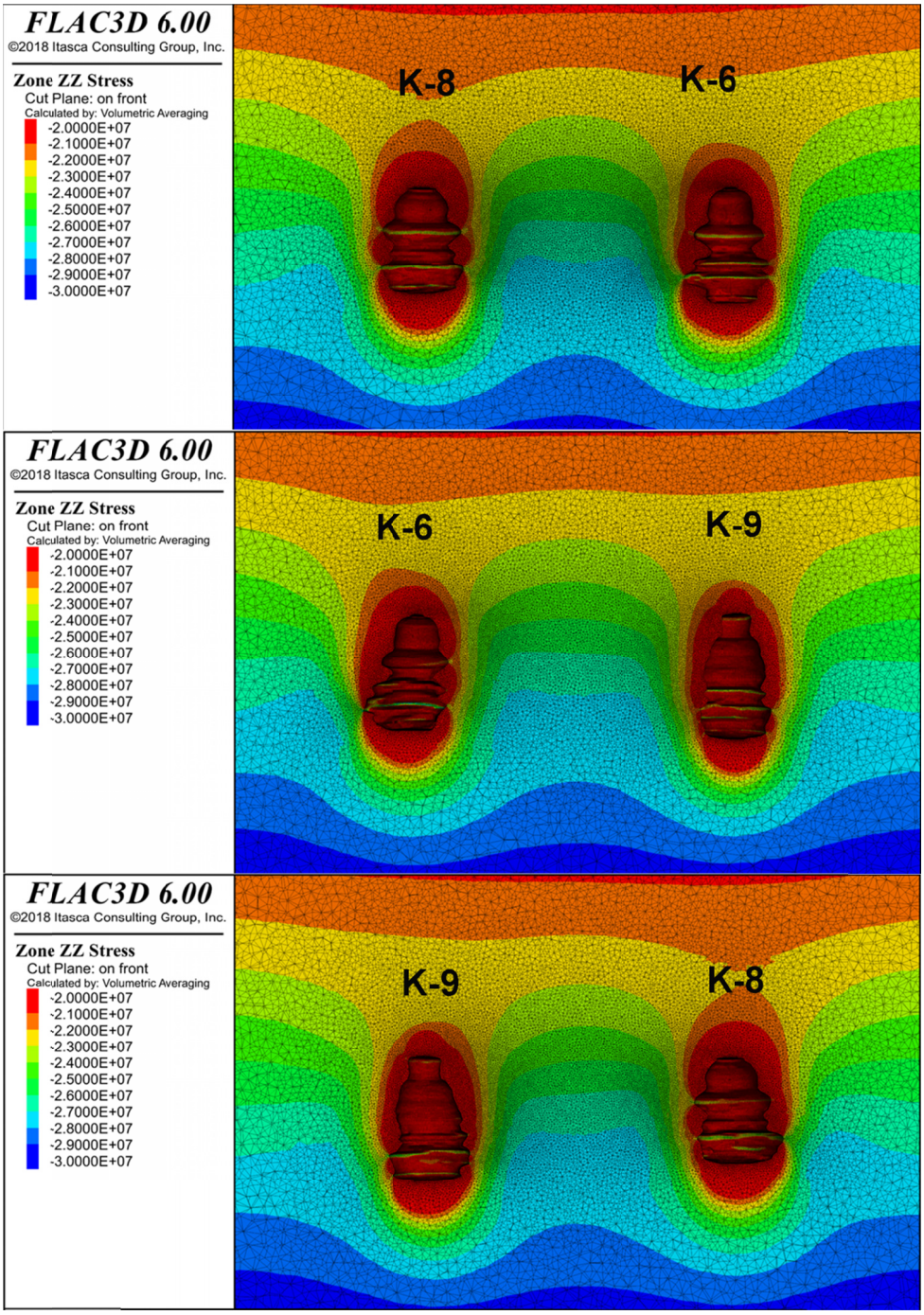

Fig. 11. Map of the vertical stress for a group of caverns at the end of the brine storage period (after 4 years). The highest values of vertical stress are marked in light green

to the zones in which the diameter of caverns changes significantly (in a vertical cross-section) and irregularities in cavern shape are visible. The maximal value of the von Mises stress in these zones is 9.0 MPa. Other areas of stress concentration, where the von Mises stress value reaches 11.4 MPa (K-8 cavern), are located below the caverns bottom, at the lower anhydrite layer (A1d).

In the numerical calculations performed for the group of all three caverns, the expected values of the von Mises stress are higher than determined in the analysis performed for each cavern separately, and locally reach 25.0 MPa at the end of the brine storage period (Fig. 10). The higher von Misses stress value results from different conditions during the performed numerical calculations. In the numerical analysis performed for the group of caverns, the interaction between the caverns and the additional stress concentrations were assumed.

Moreover, the maximum vertical stress determined for the group of the three analysed caverns amounts to 30.0 MPa at the end of the completion period and 26.0 MPa at the end of the brine period. The indicated areas, characterised the by maximal value of the vertical stress, are connected with the changes in the shape of the caverns. It was indicated that stress is concentrated in these areas where a cavern diameter changes within a few meters (in the vertical cross-section). The determined areas are more extensive in the first period (immediately after leaching). On the map (Fig. 11) there are five zones associated with the irregularities in the shape of caverns, including the contact between rock salt and anhydrite interbeds. In the second period (brine storage period), there are three areas associated with contact zones.

In addition, the convergence for all caverns was calculated. The rate of convergence in the studied caverns was the highest (0.6%) immediately after leaching and gradually decreased with time. The average convergence at the end of the brine storage period is expected to reach 1.63%. At the end of operation period (after 9.5 years), the predicted convergence of each cavern amounts to: 4.82% for the K-9 cavern, 4.68% for the K-6 cavern and 4.46% for the K-8 cavern.

Finally, the strength/stress ratio, which is considered being a safety factor, in the rock mass surrounding the caverns was analysed for each cavern. The strength/stress ratio ranged from 3.5 to 4 at sidewalls of caverns, however this value locally dropped to 2.5. The low value of the safety factor is associated with the area where a shape of caverns is irregular (Fig. 12). The results determined for each cavern were confirmed by an analysis performed for the group of all three caverns (Fig. 13).

5. Conclusions

The results of the 3D numerical modelling had indicated that the stability and integrity of the analysed caverns are not expected to be affected in the assumed operation conditions and time period (9.5 years). The strength/stress ratio (considered as a factor of safety) in the rock mass surrounding the analysed caverns is predicted to reach 3.5-4.0. In the areas where the shape of caverns is irregular, the strength/stress ratio decreases to 2.5. However, these areas occur locally and are associated with the completion period (immediately after leaching). Consequently, these local decreases, when considered as a factor of safety, are not expected to have a significant influence on the long term stability of the caverns.

The predicted distribution of the von Mises stress that is equivalent to the primary and the secondary creep rate is differentiated within the rock salt and the nonsalt rocks surrounding the analysed caverns. The highest value of the von Mises stress is associated with the lower anhydrite

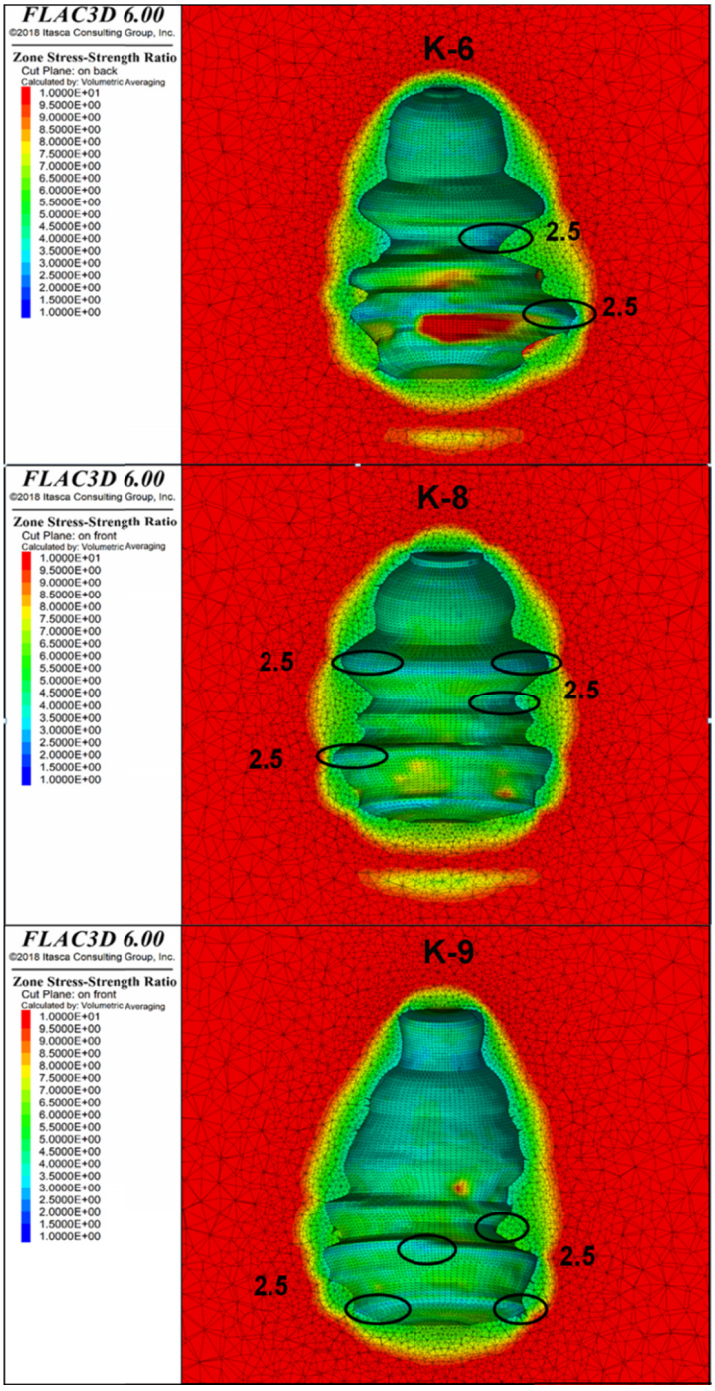

Fig. 12. Map of strength/stress ratio for each cavern immediately after leaching. Areas with low strength/stress ratio are circled in black

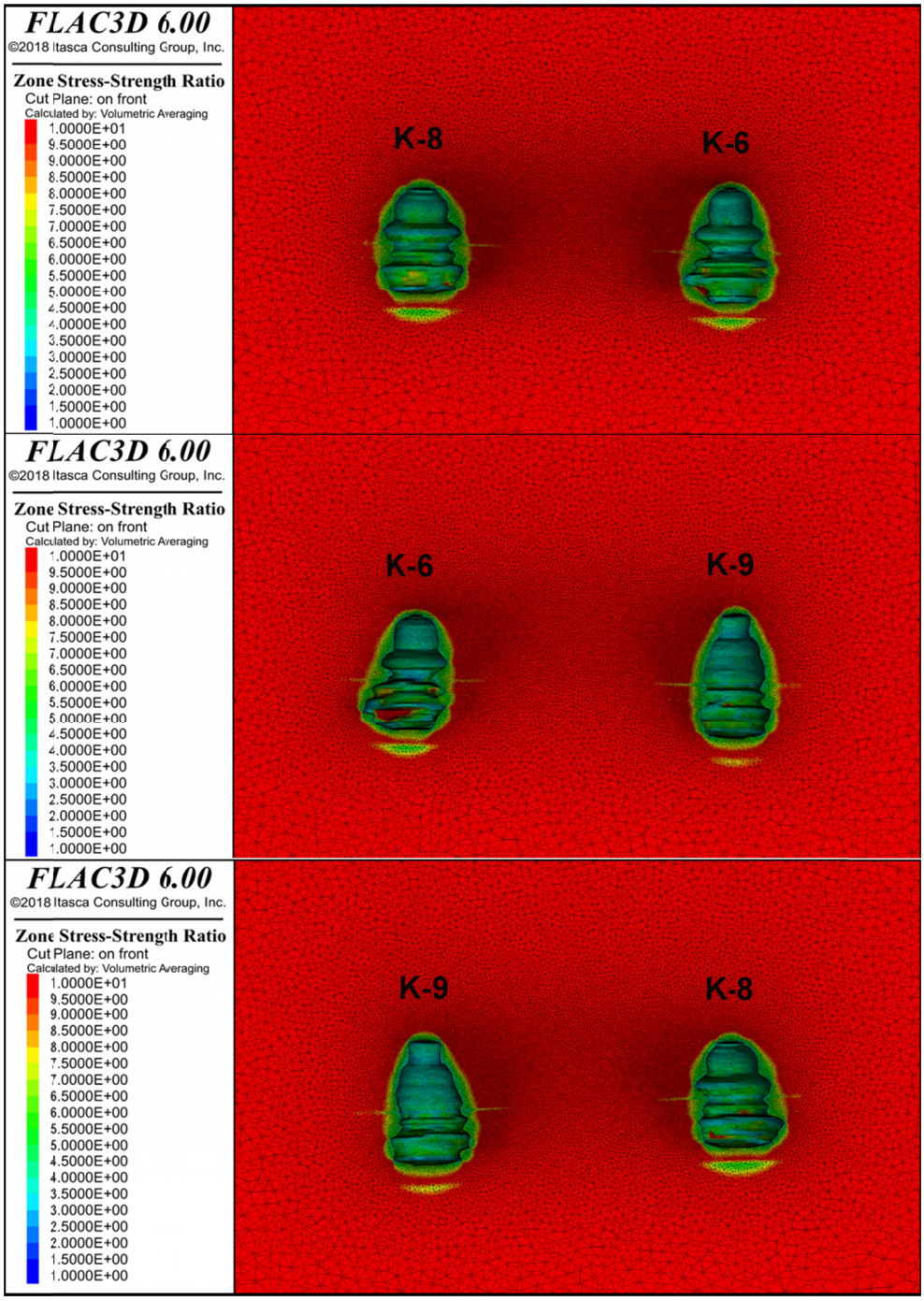

Fig. 13. Map of strength/stress ratio for the group of caverns immediately after leaching. Low strength/stress ratio areas are marked in dark blue

layer below the bottom of the caverns. The high value of the von Mises stress is associated with the irregularities in the cavern geometry where the diameter changes significantly (in a vertical cross-section) within a few meters. The irregular geometry of the caverns, simulated in numerical models, results in stress concentrations (deVries et al., 2005). These irregularities are associated with the contact between the rock salt and the anhydrite interbeds. It was assumed that the intersection locations between the rock salt and the nonsalt interlayers are prone to a stress concentration (Wang et al., 2016). Moreover, the high values of the vertical stress, which represents the overburdening pressure on the analysed caverns, correspond with the irregularities in a shape of caverns.

The displacement values at the sidewalls of the caverns are differentiated. It is clearly visible that the maximum displacements correlate with the contact area between the rock salt and the anhydrite interbeds. These contact areas are prone to discontinuous deformations, caused by the different mechanical properties of the rock salt and the nonsalt rocks. The discontinuous deformations can contribute to the migration of stored substances e.g. gas (Xiong et al., 2015). Although in the analysed caverns the indicated areas of maximum displacements occur locally, they should be considered as a potentially dangerous factor in assessing the long-term integrity of the caverns.

The expected convergence rate calculated in this study is the highest immediately after the leaching. The convergence rate is predicted to reach 5% during the operation period (after 9.5 years). Generally, the convergence rate for the caverns located at the depth of 1000-1400 m is below 1% of the cavern volume per year (Evans & Chadwick, 2009). Consequently, the convergence rate predicted for the analysed caverns in the Mechelinki salt deposit is much lower.

To conclude, the occurrence of anhydrite interbeds within the rock salt beds had contributed to the reduction in a diameter and irregular shape of the analysed caverns. The contact area between the rock salt beds and the anhydrite interbeds is prone to the concentration of stress and the occurrence of displacements. Therefore, the numerical modelling results described in this paper confirm that the anhydrite interbeds have an effect on the cavern stability.

Acknowledgement

The authors would like to thank Gas Storage Poland sp. z o.o. for making the data about the caverns available for analysis and publication.

References

Brańka S., Kasprzyk W., Piesiewicz T., Rybka J., Urbańczyk K., 2014. *Planned K-6, K-8, K-9 caverns – project of shape, volume and storage pressure*. CHEMKOP report, Cracow.

Bruno M.S., 2005. *Geomechanical analysis and design considerations for thin-bedded salt caverns: final report*. Arcadia, CA: Terralog Technologies USA.

Bruno M.S., Dorfmann L., Han G., Lao K., Young J.T., 2005. *3D geomechanical analysis of multiple caverns in bedded salt*. In: SMRI Fall Meeting, October 1-5, 2005, Nancy, France, 1-25.

Cosenza P., Ghoreychi M., Bazargan-Sabet B., de Marsily G., 1999. *In situ rock salt permeability measurement for long term safety assessment of storage*. International Journal of Rock Mechanics and Mining Sciences **36**, 4, 509-526.

Cosenza P., Ghoreychi M., 1999. *Effects of very low permeability on the longterm evolution of a storage cavern in rock salt*. International Journal of Rock Mechanics and Mining Sciences **36**, 527-533.

Czapowski G., Bukowski K., 2010. *Geology and resources of salt deposits in Poland: the state of the art*. Geological Quarterly **54**, 4, 509-518.

Czapowski G., Chełmiński J., Tomaszczyk M., Tomassi-Morawiec H., 2007. *Metodyka modelowania przestrzennego budowy geologicznej osadowych złóż pokładowych na przykładzie cechsztyńskiego złoża soli kamiennej Mechelinki nad Zatoką Pucką*. Przegląd Geologiczny **55**, 8, 681-689.

DeVries K.L., Mellegard K.D., Callahan G.D., Goodman W.M., 2005. *Cavern roof stability for natural gas storage in bedded salt*. Topical Report RSI-1829 DE-FG26-02NT41651, RESPEC, Rapid City, USA.

Evans D.J., Chadwick R.A., 2009. *Underground Gas Storage: Worldwide Experiences and Future Development in the UK and Europe*. Geological Society Special Publication 313, 1-283.

Han G., Bruno M., Lao K., Young J., 2007. *Gas storage and operations in single bedded salt caverns: stability analyses*. SPE Production & Operations, SPE-99520-PA

Jing L., 2003. *A review of techniques, advances and outstanding issues in numerical modelling for rock mechanics and rock engineering*. International Journal of Rock Mechanics & Mining Sciences **40**, 283-353.

Lankof L., Polański K., Ślizowski J., Tomaszewska B., 2016. *Possibility of energy storage in salt caverns*. AGH Drilling, Oil, Gas **33**, 2, 405-415.

Li J.P., Shi X., Yang C., Li Y., Wang T., Ma H., Shi H., Li J., Liu J., 2017. *Repair of irregularly shaped salt cavern gas storage by re-leaching under gas blanket*. Journal of Natural Gas Science and Engineering **45**, 848-859.

Li Y.P., Yang C.H., Qian Q.H., Wei D.H., Qu D.A., 2007. *Experimental research on deformation and failure characteristics of laminated salt rock*. In: Wallner M., Lux K.H., Minkley W., Hardy Jr. H.R (eds.), Proceedings of the 6th Conference on the Mechanical Behaviors of Salt, Taylor & Francis Group, London, 1-6.

Li M., 2015. *Numerical modelling investigations on waste disposal salt caverns*. Msc Thesis, Department of Civil and Environmental Engineering, University of Alberta, Canada.

Minkley W., Muhlbauer J., 2007. *Constitutive models to describe the mechanical behavior of salt rocks and the imbedded weakness planes*. In: Wallner M., Lux K.H., Minkley W., Hardy Jr. H.R (eds.), 6th Conference on the Mechanical Behaviors of Salt; Taylor & Francis Group, London, 119-126.

Sobolik S.R., Ehgartner B.L., 2006. *Analysis of shapes for the strategic petroleum reserve*. Albuquerque, USA: Sandia National Laboratories.

Swift G.M., Reddish D.J., 2005. *Underground excavation in rock salt*. Geotechnical and Geological Engineering **23**, 1, 17-42.

Wang T., Yan X., Yang H., Yang X., Jiang T., Zhao S., 2013. *A new shape design method of salt cavern used as underground gas storage*. Applied Energy **104**, 50-61.

Wang T., Yang C., Ma H., Li Y., Shi X., Li J., Daemen J.J.K., 2016. *Safety evaluation of salt cavern gas storage close to an old cavern*. International Journal of Rock Mechanics & Mining Sciences **83**, 95-106.

Warren K., 2006. *Evaporites, sediments, resources and hydrocarbons*. Springer-Verlag Berlin Heidelberg.

Wilkosz P., Burliga S., Grzybowski Ł., Kasprzyk W., 2012. *Comparison of internal structure and geomechanical properties in horizontally layered Zechstein rock salt*. W: Bérest P., Ghoreychi M., Hadj-Hassen F., Tijani M. (eds.): Mechanical Behavior of Salt VII. Leiden, CRC Press, Taylor & Francis Group, 89-96.

Xiang J., Huang X., Ma H., 2015. *Gas leakage mechanism in bedded salt rock storage cavern considering damaged interface*. Petroleum **1**, 4, 366-372.

Yang C.H., Liang W.G., Wei H.D., 2005. *Investigation on possibility of energy storage in salt rock in China*. Chinese Journal of Rock Mechanics and Engineering **24**, 4409-4417.

Yu L., Liu J., 2015. *Stability of interbed for salt cavern gas storage in solution mining considering cusp displacement catastrophe theory*. Petroleum **1**, 1, 82-90.

Zhang G., Wu Y., Wang L., Zhang K., Daemen J.J.K., Liu W., 2015a. *Time-dependent subsidence prediction model and influence factor analysis for underground gas storages in bedded salt formations*. Engineering Geology **187**, 156-169.

Zhang G., Li Y., Daemen J.J.K., Yang C., Wu Y., Zhang K., Chen Y., 2015b. *Geotechnical feasibility analysis of compressed air energy storage (CAES) in bedded salt formations: a case study in Huai'an City, China*. Rock Mechanics and Rock Engineering **48**, 5, 2111-2127.